IEEE Access
Multidisciplinary | Rapid Review | Open Access Journal

Received November 11, 2021, accepted December 7, 2021, date of publication December 16, 2021,
date of current version December 28, 2021.

Digital Object Identifier 10.1109/ACCESS.2021.3136174

Model Predictive Control-Based Thermoelectric Cooling for Rough Terrain Rescue Robots

MAYUR KISHORE, BIBHU SHARMA, BRANESH M. PILLAI, (Member, IEEE), AND JACKRIT SUTHAKORN, (Member, IEEE)
Center for Biomedical and Robotics Technology (BART LAB), Faculty of Engineering, Mahidol University, Salaya, Nakhon Pathom 73170, Thailand

Corresponding author: Jackrit Suthakorn (jackrit@bartlab.org; jackrit.sut@mahidol.ac.th)

This work was supported in part by the East Asia Science and Innovation Area Joint Research Program (e-ASIA JRP) Grant through the National Science and Technology Development Agency (NSTDA) and Mahidol University, Thailand, under Grant P-19-50869.

ABSTRACT The problem of cooling in rescue robots is similar to that of the entire domain of product development involving electronic systems. When considering mission-oriented rescue robots, this issue becomes more severe, as the tolerance to failure is remarkably low. While cooling is considered indispensable, the hazardous environmental condition of the scene of deployment, comprising of water, dust, toxic gases, or fire, constrains the choices of the method. Hence, the usage of the atmospheric air intake for cooling purposes, which is prevalent among conventional cooling systems within robotics and electronics, may not be viable, demanding a control-volume cooling system. However, such methods involving active elements might be detrimental to energy consumption and ultimately to the rescue mission, since robots in these scenarios have to operate with limited energy availability. Therefore, considering these particular problems associated with rescue robots, this paper introduces and discusses the relevance of thermoelectric cooling in rescue robot systems employed in real-time rescue scenarios. Furthermore, to optimize the energy consumption cost, this paper proposes the use of Model Predictive Control (MPC) as the appropriate temperature control method for the thermoelectric element. The analysis includes Computational Fluid Dynamics (CFD)-based cooling analysis of the robot along with the comparative analyses of uncontrolled cooling and controlled cooling under different available control methods. The results suggest sufficient cooling performance along with optimum energy consumption for the proposed model when compared with other available scenarios, based on different parameters of performance.

INDEX TERMS Heat transfer, model predictive control, terrain robot, temperature control, thermoelectric cooling.

I. INTRODUCTION

One of the primary applications of rescue robots has been to serve as the first responders during natural or man-made disasters [1]–[4]. They are supposed to execute certain tasks such as searching the victims, mapping the environment, manipulating the environment, providing limited medical intervention, etc. Generally, the disaster sites pose intricacies regarding access, which can be addressed effectively through the application of multi-agent robots [5]. The communication and co-ordination eases the transfer of information between the robots having different modes of mobility, sensor and structure [6].

The associate editor coordinating the review of this manuscript and approving it for publication was Yingxiang Liu.

While environment comprises of certain challenges, the rescue robots which operate in land, air or water have limited margin for failure. Failure of one component could jeopardize the overall search and rescue operation, which is basically a race against the time [7], [8]. Although several of the components are susceptible to failure, the failure involving electronic components is definitely challenging to counteract. Besides, it is stated that more than 55% of the electronic failures occur because of the high temperature [9].

Therefore, most of the electronic devices including robots have a provision for a relevant thermal management system. Most of the popular thermal management systems such as forced air/liquid cooling systems, heat pipes, phase change materials (PCM), are not quite reliable for the rescue robots [10]–[12]. First of all, the rough terrain might inflict

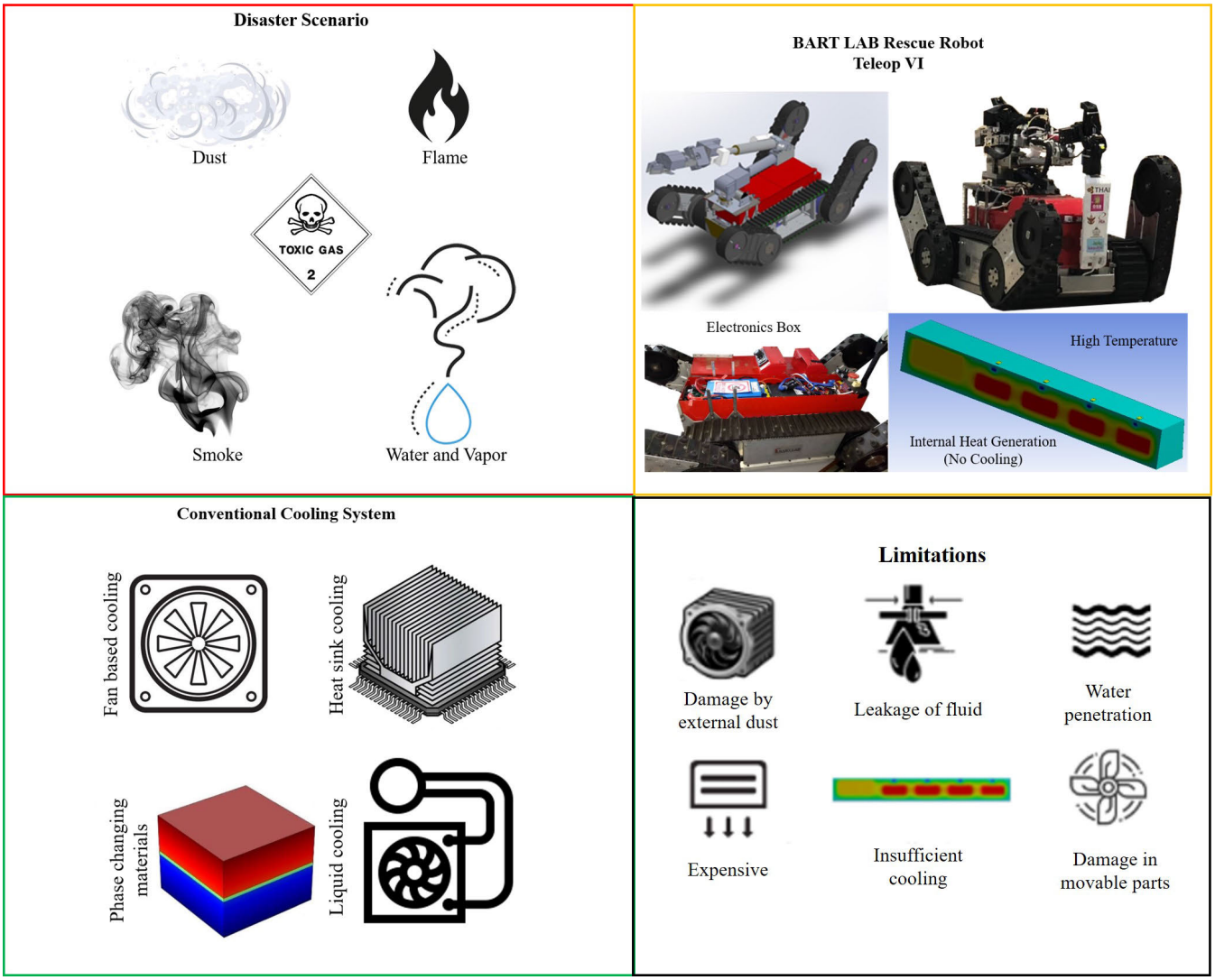

FIGURE 1. **Overview of Thermal Management in Rescue Robot.**

severe impact on the robot that may induce leakage. Besides, during these conditions, especially in the case of chemical hazards, conventional forced cooling technique facilitated by the surrounding air results in the entry of foreign airborne substances and harmful gases giving rise to the failure of electronic parts which could ultimately result in the failure of robot and even sabotage the rescue mission. Hence, in contrast to the conventional robots, a particular method is being proposed for rescue mission robots. Moreover, from the experience of the rescue operations, it is recommended for these robots to be waterproof [13]–[15].

The majority of the cooling systems discussed are not effective for rescue robots due to some fundamental difference between rescue robots and normal robots regarding the field of application. Regarding the majority of the conventional robots, the working environment is known and the risk factor in conventional cooling is sufficiently low for smooth operation. Whereas in the case of rescue robots the operating environment is harsh, unpredictable and severely detrimental for the performance and the integrity of the robot.

One of the appropriate solutions to the problem has been the use of thermoelectric cooler (TEC) [10], [16]–[18]. Thermoelectric cooling is a technique which uses the Peltier effect to create a heat flux at the junction of two different types of materials [19], [20]. A Peltier cooler is a solid-state active heat pump which transfers heat from one side of the device to the other, with consumption of electrical energy, depending on the direction of the current [21], [22]. Compared to the conventional method, TEC does not require atmospheric air and moving parts for operating. Thus, the system avoids any vibration and noise. Moreover, the system offers relatively precise control over the temperature [23], [24].

However, the effectiveness of TEC is unambiguously dependent over the control technique [25]. The selection of control technique is an agreement between performance, precision, response time, steady state error, etc. For instance,

PID control has been widely used in temperature control operation of TEC [26]–[28] because it offers simple yet dynamic solution. This research uses model predictive control (MPC) to control the behaviour of the TEC. [29] has used similar control system within a heat pump involving thermoelectric material. Compared to PID control, MPC allows time-dependent non-linear parameters and also offers optimization along some cost function [30]–[32]. The main aim of using this control system with the rescue robot is precise set point control through minimum energy usage [33].

The BART LAB (Center for Biomedical and Robotics Technology), Faculty of Engineering, Mahidol University, has been involved with rescue robots since 2006. The team has participated in national and international robot competitions and has also been acquainted with the actual disaster scenarios [34]. The team is relentlessly pursuing the research and development of rescue robots regarding the control, hardware, sensor-fusion and communication [35]–[37]. One of the perennial observations throughout the tests in various scenarios has been the susceptibility of electronic box (housing for processor, motor drivers and other electronic parts) to fail due to the accumulated dust attributed to the atmospheric air intake by the cooling fan. An overview of the problem is illustrated in Fig.1. In order to overcome the scenario, thermoelectric coolers are introduced as the cooling element such that the electronic box is isolated from the ambience without hindering cooling (Fig. 2). With the implementation of an optimization-based control model as that of MPC [38], [39], we aim to obtain an effective cooling performance with the optimum energy consumption (Fig.3).

Specifically, the contributions of this paper towards the scientific literature can be summarized as

- Introducing an alternative control-volume cooling based on thermoelectric coolers within the area of rescue robotics
- Incorporating energy optimized MPC for thermoelectric cooling in rescue robot and comparing the performance with prevalent PID control system for cooling
- Conducting Computational Fluid Dynamics (CFD) analysis of robot from the perspective of temperature for problem identification and solution optimization.

The method section would elaborate the mathematical model of TEC for representing within the MPC. The material and methods of the analysis would be delineated in the simulation section, followed by the discussion and comparative study in the result section.

II. METHODS

In regards to MPC, the validity of the model plays significant role for accuracy and consistency. The mathematical model for this system should incorporate all the heat transfers including the model of thermocouple. From equations (1)-(10), state-space model is developed, which would form the basis for the MPC algorithm.

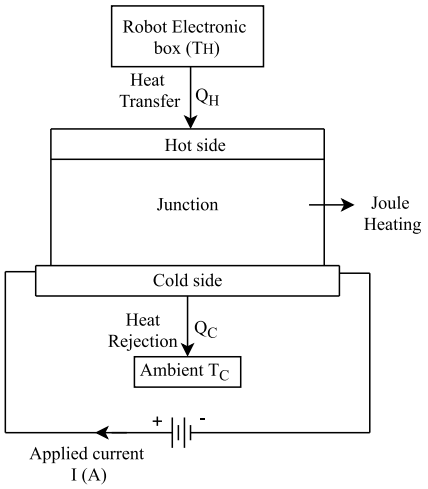

FIGURE 2. Concept of a thermoelectric cooling system.

A. THERMOELECTRIC HEAT TRANSFER MODEL

The holes in the p-type semiconductor and the electrons in the n-type semiconductor migrate from the cold end to the hot end when current flows from the p-type semiconductor to the n-type semiconductor are applied, the corresponding Peltier heats will be produced at the interface between connectors and semiconductors [18]. The heat is absorbed at the cold end and emitted by the Peltier effect at the hot end, producing a temperature difference of $T_H - T_C$. Owing to Fourier's heat conduction, the heat would be transferred from the hot end to the cold end with the temperature difference. The final cooling power of the TEC, Q_C, is thus determined by the combined effect of heat from Peltier, Fourier's heat conduction, Joule heat, and Thomson heat. The physical model of the system has been illustrated in Fig. 2.

The linear dynamic model is designed by considering the working components of thermoelectric cooler,in which the first component is Peltier effect

$$Q_p = \alpha I T \tag{1}$$

where α is the Seebeck Coefficient, T is the temperature of the corresponding hot/cold side and I is the applied current through TEC. Another component, Joule heating, which is the heating resulted from the current passing through the thermocouple, can be illustrated as

$$Q_j = \frac{1}{2} I^2 R \tag{2}$$

where R is the electrical resistance of thermoelectric module. The third component is the thermal conduction of the semiconductor material which can be defined by the equation (3).

$$Q_f = k \Delta T \tag{3}$$

Thus the heat flux at cold side Q_c and hot side Q_h can be determined through equation (1), (2), and (3)

$$Q_c = \alpha I T_c - \frac{1}{2} I^2 R - k \Delta T \tag{4}$$

$$Q_h = \alpha I T_h + \frac{1}{2} I^2 R - k \Delta T \tag{5}$$

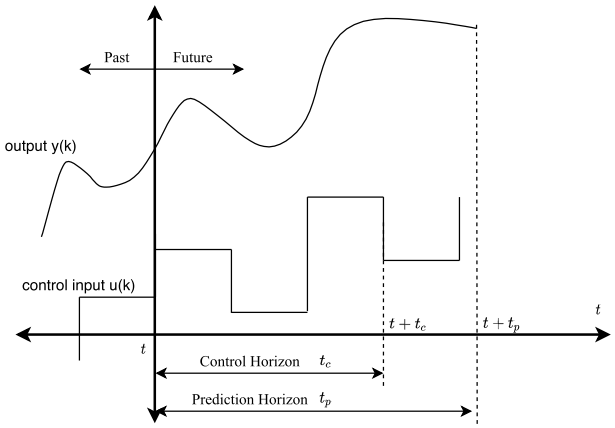

FIGURE 3. Overview of MPC.

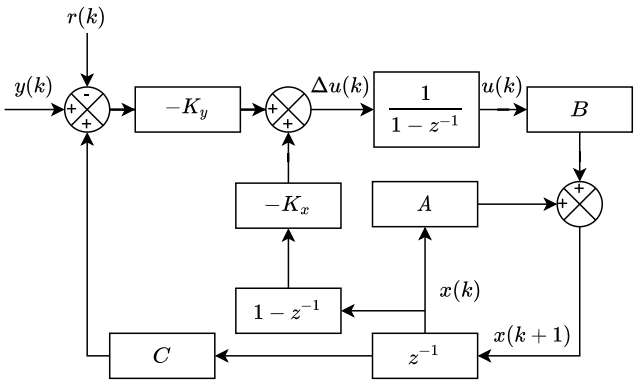

FIGURE 4. The MPC block diagram representation.

The fourth component which is the heat flux from heat exchanger to the TEC module and from TEC module to heat exchanger can be represented through convective heat transfer model as

$$\dot{Q} = hA(T_1 - T_2) \tag{6}$$

where h is the thermal conductivity of the boundary medium, A is the contact surface area between two thermal bodies and T_1 and T_2 are the temperature across fluid and solid medium. Therefore, the net heat flux at cold side can be illustrated as

$$\dot{Q}_{totC} = \dot{Q}_{comp} - \dot{Q}_c \tag{7}$$

which when expanded according to the relevant terms becomes

$$\dot{Q}_{totC} = hA(T_{comp} - T_C) - \alpha I T_C + \frac{1}{2} I^2 R + k(T_C - T_H) \tag{8}$$

Similarly, the net heat flux at hot side can be represented as

$$\dot{Q}_{totH} = \dot{Q}_H - \dot{Q}_{out} \tag{9}$$

which can be elaborated as

$$\dot{Q}_{totH} = \alpha I T_C + \frac{1}{2} I^2 R - k(T_C - T_H) - hA(T_{out} - T_C) \tag{10}$$

The equations (8) and (10) are the state-space model, which are also similar to the state-space model developed in [29] and [18].

B. MPC BASED MODELING

Model Predictive Control (MPC) is based on the prediction of the future trajectory of the control variable $u(k)$ to achieve the optimum output $y(k)$. As this prediction is bound within a finite future time, the method is also termed as receding horizon control method. With the progression of the time, the moving horizon is updated with the same interval. The core of the MPC method is the construction of the mathematical model of the plant [40]. For obtaining the model of the process, several algorithms such as Dynamic Matrix Control, Model Algorithmic Control, Predictive Functional Control, Extended Prediction Self Adaptive Control, Generalized Predictive Control, and State Space Formulation are generally preferred [41]. Among these, State Space Formulation offers several attributes that are relevant to this problem. While constructing prediction model from methods such as transfer model can be intricate, for state-space model the task is unambiguous [42]. Similarly, the model offers ease when extending to multi-variable system or a non-linear system from a linear one [41].

The state-space model of the plant is used to predict the future variable based on the current value of the state variable $x(k)$. As such, the behaviour can be summarised as

$$x(k+1) = Ax_m(k) + Bu(k) \tag{11}$$

$$y(k) = Cx(k) \tag{12}$$

where, A, B and C are called the augmented model. These are based on the discrete-time model, which are convenient from the practical perspective. Fig. 3 illustrates the basic understanding of the MPC which comprises of the essential parameters involved in the system.

In Fig. 3, t_p refers to the prediction horizon whereas t_c refers to the control horizon. The future outputs are predicted until the prediction horizon whereas, future control signals prediction is constrained until the control horizon. The prediction of control signal is facilitated by optimization to minimize the error between the reference trajectory and the current measurement. This determination can be simplified if the objective function of optimization is quadratic and the model is linear. From this model, explicit solution can be extracted [41].

From the equations (11) and (12), future state variable $x(k+1|k)$ can be calculated from future control parameter $\delta u(k)$ within the control horizon as

$$x(k+1|k) = Ax(k) + B\Delta u(k) \tag{13}$$

and so forth. Subsequently, the output variable can also be predicted as

$$y(k+1|k) = CAx(k) + CB\Delta u(k) \tag{14}$$

TABLE 1. Simulation parameters of TEC module.

Property	Bi_2Te_3	Copper
Density,kg/m^3	7740	8920
Thermal conductivity,W/k-m	1.6	350
Specific heat capacity,J/k-kg	154.4	385
Electrical conductivity,S/m	1.1×10^5	5.9×10^8
Seebeck coefficient,V/K	$\pm 200 \times 10^{-6}$	6.5×10^{-6}

for all k within the predicted horizon. All the terms within the respective horizons can be accumulated and simplified similar to [40] as

$$Y = Fx(k) + H\Delta U \tag{15}$$

where, F and H consists of the respective combinations of the augmented model (A, B, C). This obtained model is then optimized such that the error between set-point signal $r(k)$ and the predicted output is minimized. This synthesis further ensures the determination of the optimum control parameter for the minimum error. This is performed through minimization of a cost function $J(k)$ [29] such that

$$J(k) = \sum_{i=1}^{T_p} y(i|k) + \sum_{i=0}^{T_c-1} y(i|k) \tag{16}$$

The equation (16) can be rewritten in terms of R_s (set-point vector $r(k)$ in frequency domain), and minimized with respect to ΔU to determine the optimum control signal as [40]

$$\Delta U = (H^T H + \bar{R}^{-1} H^T (\bar{R}_s r(k) - Fx(k)) \tag{17}$$

Thus, by determining H^TH, $H^T F$ and $H^T \bar{R}_s$, the MPC can be implemented to determine the optimum control for improved performance of the system. From the model, a block diagram can be constructed.

The terms K_x and K_y represents the feedback gain for $\Delta x(k)$ and $y(k)$ respectively. Similarly, z^{-1} represents delay and $1/(z-1)$ represents discrete-time integrator. In this paper, the state-space model represented by equation (8) and (10) has been modeled using Simulink in MATLAB R2020a. Then, the MPC is implemented within the system and simulation is performed to validate the model.

III. SIMULATION AND RESULT

The models discussed in the previous section has been tested with various simulation methods. The heat transfer and thermocouple has been modeled in ANSYS Fluent-19.3 (academic license version) where the heat transfer problem was defined through the computational fluid dynamics (CFD) method. Similarly, the control model was simulated through Simulink in MATLAB R2020a with appropriate parameters.

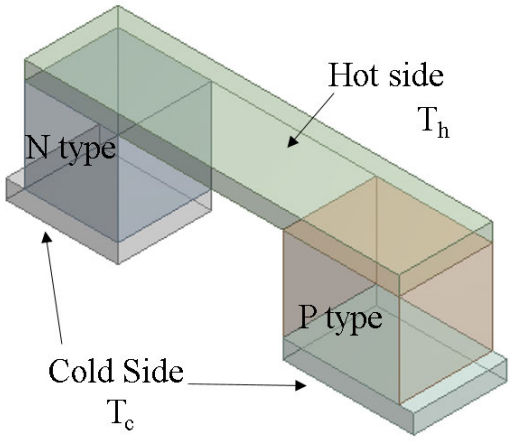

FIGURE 5. Simulation model of thermoelectric cooler.

A. CFD SIMULATION

Differential equation can be considered in case of control mass. The general form of conservation of mass can be expressed as

$$\frac{\partial \rho}{\partial t} + \frac{\partial(\rho u)}{\partial x} + \frac{\partial(\rho v)}{\partial y} + \frac{\partial(\rho w)}{\partial z} = 0 \tag{18}$$

where, ρ (Kg/m^3) denotes density, u, v and w represents velocities (m/s) in x, y and z coordinates respectively.

The conservation of momentum for x, y, z coordinates can be written as following respectively,

$$\frac{\partial(\rho u^2)}{\partial x} + \frac{\partial(\rho uv)}{\partial y} + \frac{\partial(\rho uw)}{\partial z} + \frac{\partial(\rho u)}{\partial t} = -\frac{\partial \rho}{\partial x} + \mu\left(\frac{\partial^2 u}{\partial x^2} + \frac{\partial^2 u}{\partial y^2} + \frac{\partial^2 u}{\partial z^2}\right) + \rho g_x \tag{19}$$

$$\frac{\partial(\rho uv)}{\partial x} + \frac{\partial(\rho v^2)}{\partial y} + \frac{\partial(\rho vw)}{\partial z} + \frac{\partial(\rho v)}{\partial t} = -\frac{\partial \rho}{\partial y} + \mu\left(\frac{\partial^2 v}{\partial x^2} + \frac{\partial^2 v}{\partial y^2} + \frac{\partial^2 v}{\partial z^2}\right) + \rho g_y \tag{20}$$

$$\frac{\partial(\rho uw)}{\partial x} + \frac{\partial(\rho vw)}{\partial y} + \frac{\partial(\rho w^2)}{\partial z} + \frac{\partial(\rho w)}{\partial t} = -\frac{\partial \rho}{\partial y} + \mu\left(\frac{\partial^2 w}{\partial x^2} + \frac{\partial^2 w}{\partial y^2} + \frac{\partial^2 w}{\partial z^2}\right) + \rho g_z \tag{21}$$

where, μ is the dynamic viscosity (kg/ms), and g is the gravitational acceleration (m/s^2).

Since the system deals with internal energy generation, producing convection effect inside the box, the mathematical relation of energy has to be determined. Therefore, the energy equation can be written as [43]

$$\frac{\partial}{\partial x}(\rho ucT) + \frac{\partial}{\partial y}(\rho vcT) + \frac{\partial}{\partial z}(\rho wcT) = \frac{\partial}{\partial x}\left(k\frac{\partial T}{\partial x}\right) + \frac{\partial}{\partial y}\left(k\frac{\partial T}{\partial y}\right) + \frac{\partial}{\partial z}\left(k\frac{\partial T}{\partial z}\right) \tag{22}$$

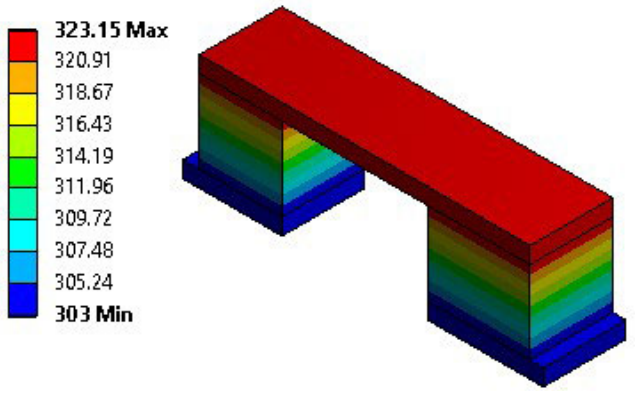

FIGURE 6. Temperature distribution in thermoelectric model.

Temperature, pressure, and velocity are all time-averaged in this simulation scenario, equation (22) is resolved for determining the energy dissipation:

$$\frac{\partial}{\partial x_i}\left(\rho k u_j\right) = \frac{\partial}{\partial x_j}\left(\mu \frac{\partial k}{\partial x_j}\right) + S_K + T \tag{23}$$

$$\frac{\partial}{\partial x_i}\left(\rho \epsilon u_j\right) = \frac{\partial}{\partial x_j}\left(\mu \frac{\partial \epsilon}{\partial x_j}\right) + S_\epsilon + T \tag{24}$$

where T is the Turbulent factor which depends on turbulence kinetic energy, turbulence kinetic energy due to buoyancy, S_k and S_ϵ are user-defined source terms. The details of the terms and constants are referred from the ANSYS-FLUENT theory book [43]. The first simulation has been performed with physical models in ANSYS. In order to validate the thermocouple model, the first analysis was performed within a single model of thermocouple as illustrated in Fig.5 [44].

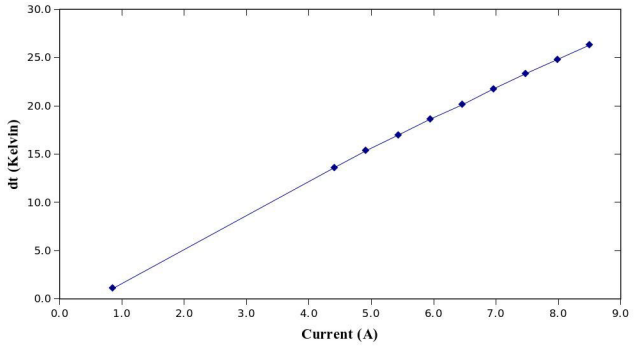

FIGURE 7. Thermocouple Behaviour Analysis (Supplied Current vs Temperature Difference).

The current was supplied within the junction made up of p-type and n-type semiconductor and the temperature difference between two sides of the unit was observed. The materials and properties chosen for the thermocouple are shown in Table 1. Except for the hot ends, all surfaces of the cooler were subjected to a convective boundary condition with a film coefficient of $h = 3$W/K/m. Fig. 6 illustrates the temperature distribution of TEC module. The value of current

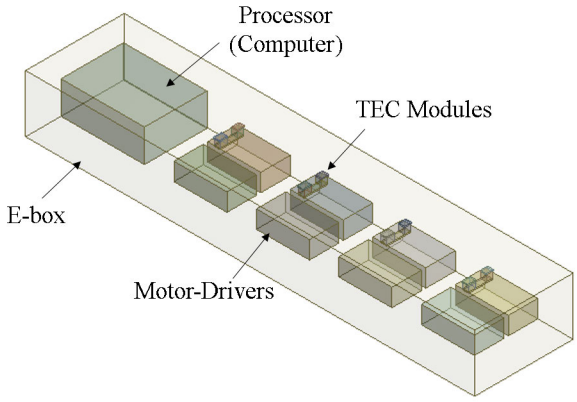

FIGURE 8. Simulation model of Terrain robot Electronic box.

TABLE 2. Analysis Settings.

Parameter	Values
No of steps	1
Step end time	$60s$
Initial step time	0.1
Minimum time step	0.05
Maximum time step	5

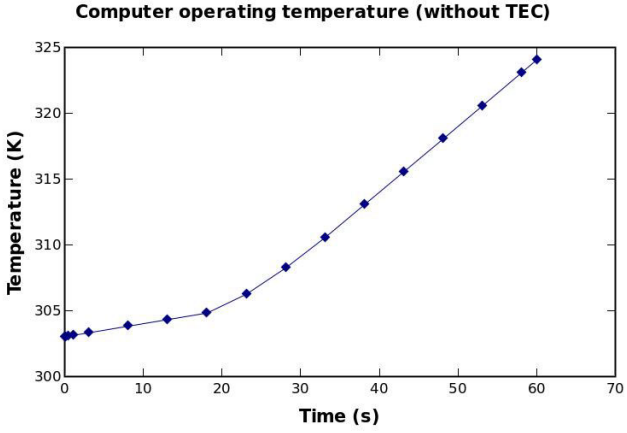

FIGURE 9. Processor temperature variation of robot without Thermoelectric cooling.

was changed and the change in difference was also observed. As Seebeck constant was considered as constant along different temperatures, a linear relation is expected between applied current and the change in temperature. The current vs temperature difference graph summarises the analysis as shown in Fig.7.

Pearson Correlation test was performed on the observed value, where the Pearson Correlation coefficient was found to be 0.999, suggesting highly linear relation. After this validation, CFD analysis was performed using this thermoelectric module and placing it within the electronic box of the real robotic system as shown in the Fig.8.

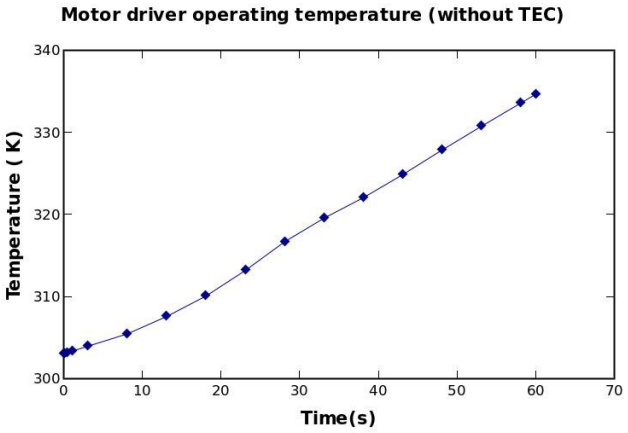

FIGURE 10. Motor driver temperature variation of robot without Thermoelectric cooling.

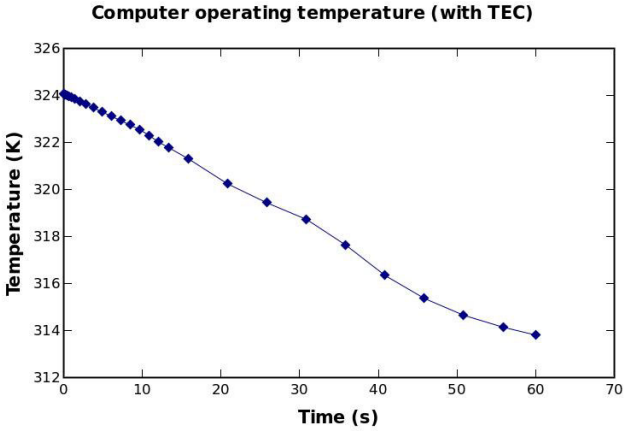

FIGURE 11. Processor temperature variation of robot with Thermoelectric cooling.

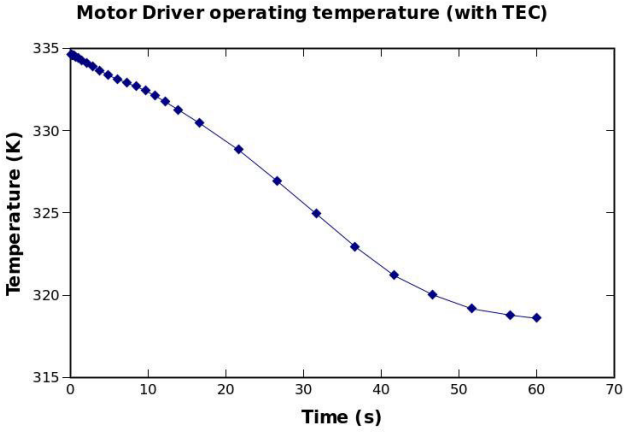

FIGURE 12. Motor driver temperature variation of robot with Thermoelectric cooling.

In this paper the CFD analysis is performed in steady state and transient state. Tetrahedral meshing was used with the average mesh size of 2mm. The ambient temperature of the

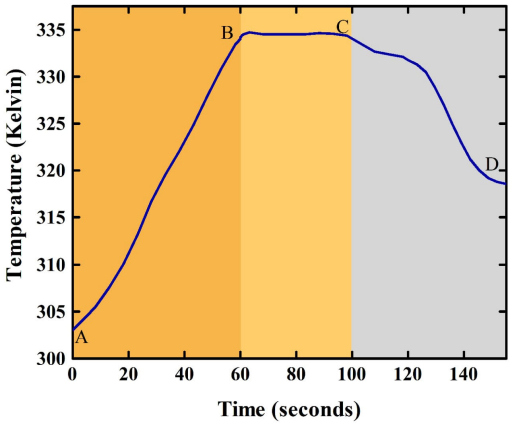

FIGURE 13. Heating and Cooling curve of robot.

analysis was taken to be 302 K and the pressure was assumed to be 1 atm. The parameters pertaining to the thermocouple has been mentioned already. The computer and motor drivers were identified to be the major heating elements of the electronic box, and the overall heat generation in the system was estimated to be 200 watt. The computer model selected for the setup is eBOX560-880-FL-4300U-EU, and the motor driver used is EPOS4 Compact 50/8 CAN. The analysis settings are as shown in Table 2. This is based on the data from the supplier of the components.

The first set of simulation without the operation of TEC was executed by considering the maximum load condition. When the operational environment temperature within the electronic box was examined individually, it was observed that the computer and motor driver temperatures exhibited a steep increasing curve trend, which was not appropriate as per the data sheet provided by the manufacturer. Fig. 9 and Fig. 10 describes the graphical representation of increase in operation temperature of both computer and motor driver respectively in which their peak temperatures was 324.06 K and 334.67 K. At temperatures such as this, there is a high probability of failure. Therefore, these kinds of robotic systems undoubtedly require thermal management scheme.

The TEC module was installed to avoid this high operating temperature, and the maximum load parameters as well as the maximum temperature exhibited in the previous simulation were assigned as the input parameters for this simulation.The overall electronic box temperature, as well as the temperature of the motor drivers and computer, were found to be 313.4 K which is within the acceptable limits after the simulation. This was achieved with the current supply of 5A across the module. Although, this is above the ambient temperature, this can be considered significantly safe when compared without the cooling case scenario. Fig.11 and Fig. 12 illustrates the effect of use of TEC modules to control the operating temperature within the permissible limits.

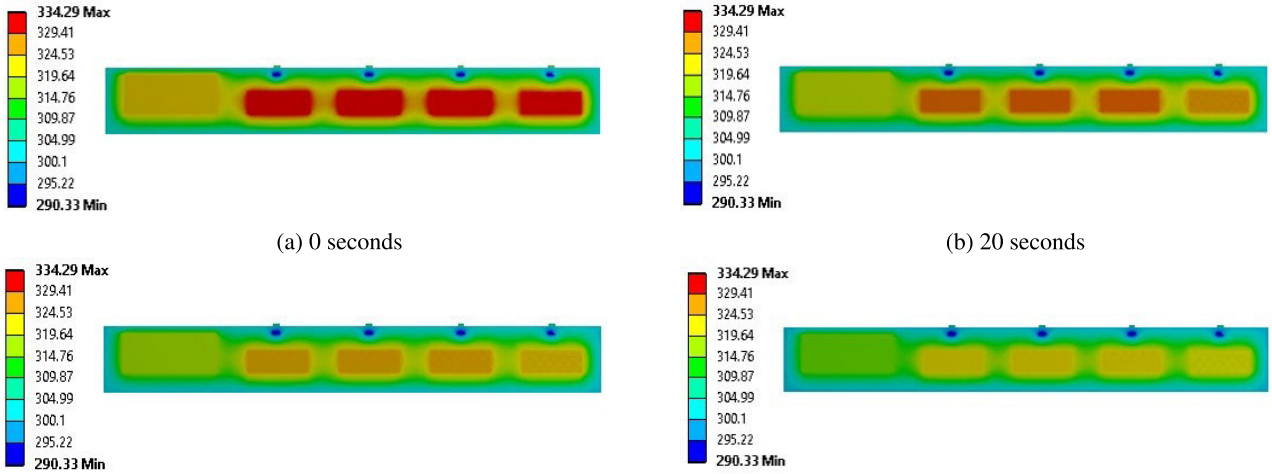

(a) 0 seconds

(b) 20 seconds

(c) 40 seconds

(d) 60 seconds

FIGURE 14. Transient temperature variation with TEC implementation.

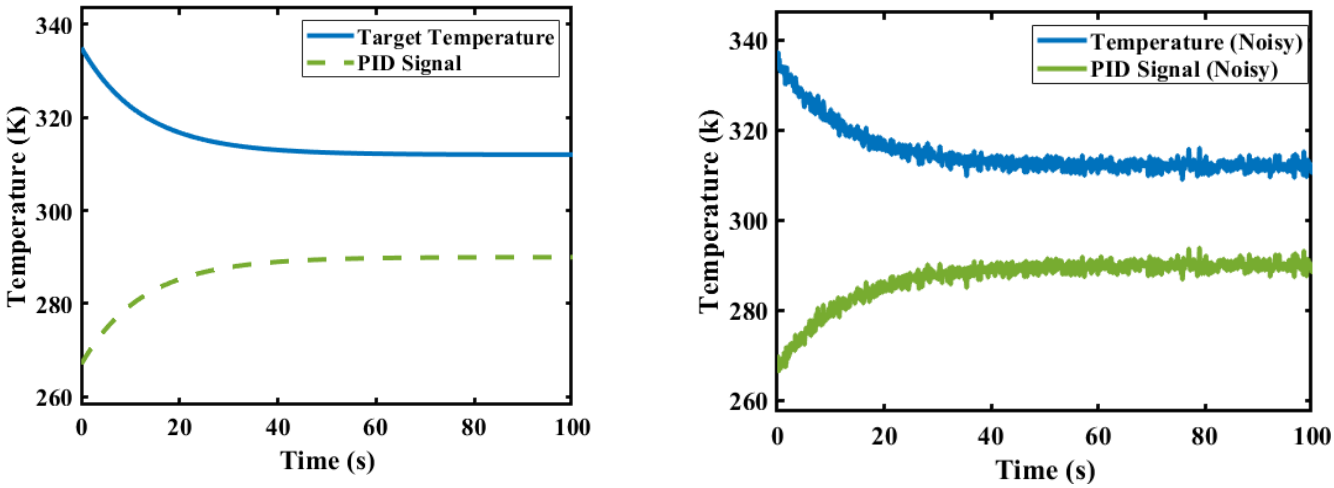

(a) Without Disturbance

(b) With Gaussian Disturbance.

FIGURE 15. Internal temperature cooling control using PID (PID signal and Output temperature).

Temperature variation of robot during different phases are shown in Fig.13. (A-B): Rise in operating temperature, (B-C): Steady state, (C-D): Cooling phase. The Fig.14a, Fig.14b, Fig.14c, and Fig.14d, shows the heat distribution contour (kelvin) within the robot at time 0, 20, 40, and 60 seconds respectively.

B. PID AND MPC SIMULATION

The simulation of the model was performed using two control methods: PID control and MPC. Using the equations of state-space, the Plant block was created in Simulink. The block consists of heating element, cooling element, conduction, convection element, thermal mass component, sensors and various signals. As temperature vs current analysis in TEC demonstrated purely linear relation from simulation (as seen in Fig. 7), temperature has been used as the control signal in this analysis. Temperature sensors are placed within the block for display and feedback. The thermal mass equivalent to the air within the electronic box of the robot has been used as the target of measurement and the simulation starts with initial temperature of the thermal mass as 320 K. Likewise, thermocouple has been modeled as a controllable temperature source, while heating elements within the system have been considered to be the heat source.

First of all, PID controller in discrete mode was used, where the gains were optimized using the transfer function method.The values were determined to be $P = 2.6$, $I = 0.42$ and $D = -1.21$. Similarly the coefficient of the filter was optimized and found to be 0.3.

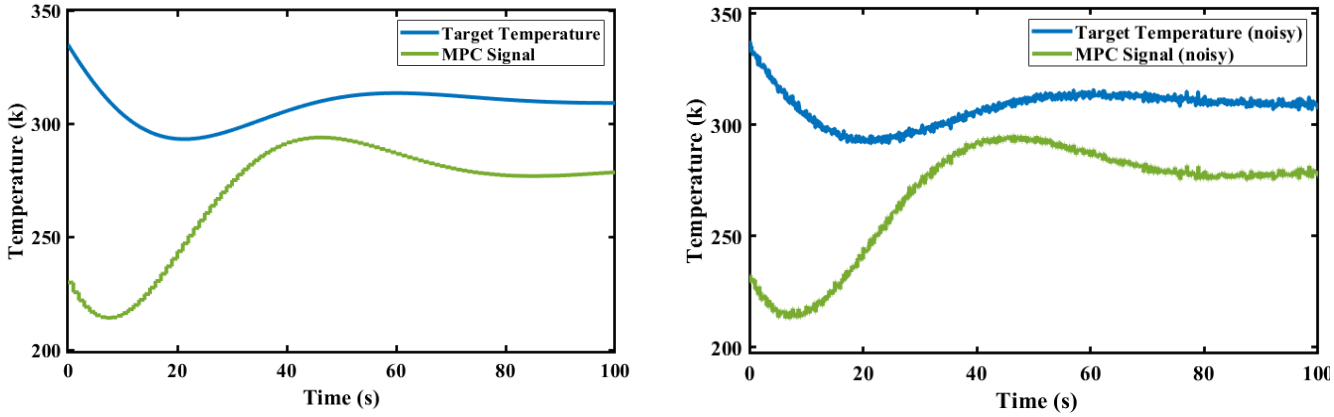

(a) Without Disturbance (b) With Gaussian Disturbance

FIGURE 16. Internal temperature cooling control using MPC (MPC signal and output temperature).

The graph demonstrates satisfactory result from the point of view of the output variable. The internal temperature of thermal mass which was initially in 320K has been reduced approximately to the supposed ambient temperature (302K) and is maintained within the limit. Similarly, the output constraint has been applied in the PID controller for the hardware limitations within the thermocouple. However, robots that traverse difficult area are susceptible to a range of thermal disturbances, which makes it imperative to test with thermal disturbances. In another analysis, disturbing signal (Gaussian white noise) was fed to the system and response of the controller was observed.

The disturbing signal produced oscillatory response, however, the system demonstrated acceptable response. However, there are several shortcomings when working with PID controller. First of all, the simulation shows that, for the system to be within the required bounds, the control signal has to be around its minima. This is concerning from the point of view of energy consumption. To maintain the thermocouple at this low temperature, significant energy has to be sacrificed, which is counterproductive for mobile robots. Therefore, MPC has been implemented and observed for better response than PID.

As compared to Fig. 15a and Fig. 15b, the MPC algorithm has better outcome. The output along with the control variable has been bound within the supposed ambient temperature. The finite horizon in the analysis has been taken as 10 seconds, while the control horizon has been considered as 2 seconds. Similarly, disturbing signal (random number signal) has also been implemented over the MPC controller. Considering the safety of the hardware, input constraint was considered to be $0 \leq I \leq 10A$. Since the MPC model allows the implementation of hard constraint and soft constraint, the hard constraint on temperature was considered to be 328K and soft constraint was assumed to be 318K.

Figure.16a and Fig.16b, depicts improved control response of the MPC with disturbance and reduction of energy consumption. Both the analyses, with and without the disturbance has demonstrated better performance from the control as well as energy point of view. Another major advantage

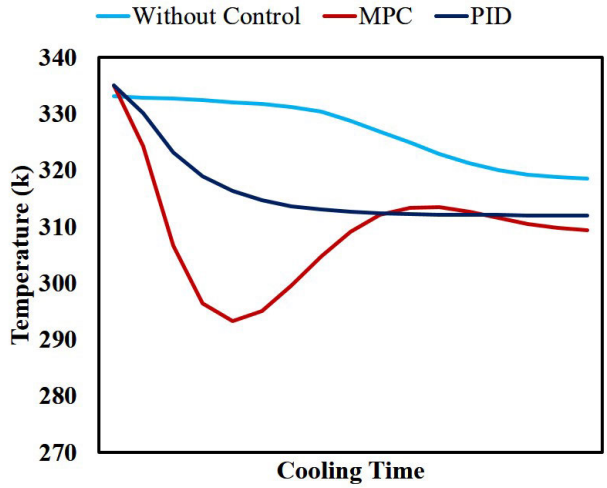

FIGURE 17. Comparison of temperature drop variation for different cooling methods.

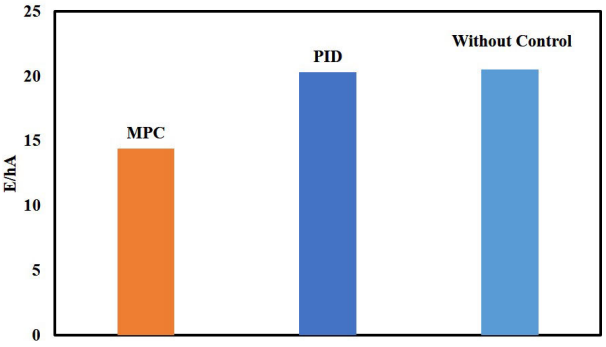

FIGURE 18. Energy cost comparison for different cooling methods.

associated with the use of MPC has been realized to be the ease of use. Although theoretically MPC pose significant challenges, from the point of view of use, MPC is quite convenient. Moreover, the tuning process in MPC is significantly convenient when compared with PID tuning which is a trivial process.

The analysis regarding the trend of cooling across different methods has been illustrated in Fig.17. The initial system temperature of 335 K, which is deemed detrimental for the robotic system, is decreased with the implementation of TEC. Without any consideration for the control system, the temperature was observed to be gradually reaching the safe zone. However, when control system such as MPC and PID were implemented, the temperature quickly reached the safe level. Moreover, the steady state temperature for controlled cooling was lower when compared with the uncontrolled cooling. This analysis highlights the requirement of appropriately controlling the TEC. The comparison is further explored through Fig.18, where energy cost of cooling is compared across the controlled and uncontrolled cooling systems. The energy cost normalized by dividing with h*area, which is common for all the methods, is plotted for various methods. This comparison highlights the justification for the use of MPC method, since it was observed to consume the least energy. For systems of this kind, energy consumption is crucial and optimum energy consumption with effective cooling is certainly a major criterion for selection.

IV. CONCLUSION

The simulation results has demonstrated promising prospect of using thermoelectric cooling with MPC based controller in robots that travel in rough environment. Since these robots suffer primarily with two constraints: limited energy availability and hazardous ambient condition, conventional cooling method is ineffective if not detrimental. This paper explored this problem and analyzed the proposed solution through CFD method and simulation methods. The CFD simulations provided substantial ground to use thermocouple along with natural convection as a cooling alternative. This contention was further corroborated by MPC analysis, which harnesses the performance and apparently facilitates the reduction in energy consumption when compared to other methods. Undoubtedly, this conclusion would still be inadequate without the physical experimentation. However, the results from the analysis is the initial step which has showed enough potential to be tested within the physical system.

ACKNOWLEDGMENT

The authors would like to express their gratitude to BART LAB Rescue Robot team members and BART LAB researchers for their contribution towards the rescue robot project, since 2006.

REFERENCES

[1] S. Opiyo, J. Zhou, E. Mwangi, W. Kai, and I. Sunusi, "A review on teleoperation of mobile ground robots: Architecture and situation awareness," *Int. J. Control, Automat. Syst.*, vol. 19, pp. 1384–1407, Oct. 2020.

[2] P. Eckert and A. J. Ijspeert, "Benchmarking agility for multilegged terrestrial robots," *IEEE Trans. Robot.*, vol. 35, no. 2, pp. 529–535, Apr. 2019.

[3] B. M. Pillai and J. Suthakorn, "Challenges for novice developers in rough terrain rescue robots: A survey on motion control systems," *J. Control Sci. Eng.*, vol. 2019, pp. 1–12, Jun. 2019.

[4] M. Li, H. Zhu, S. You, L. Wang, and C. Tang, "Efficient laser-based 3D SLAM for coal mine rescue robots," *IEEE Access*, vol. 7, pp. 14124–14138, 2019.

[5] N. Teslya, A. Smirnov, A. Ionov, and A. Kudrov, "Multi-robot coalition formation for precision agriculture scenario based on Gazebo simulator," in *Proc. 15th Int. Conf. Electromech. Robot. Zavalishin's Readings*, 2020, pp. 329–341.

[6] J. Ota, "Multi-agent robot systems as distributed autonomous systems," *Adv. Eng. Informat.*, vol. 20, no. 1, pp. 59–70, Jan. 2006.

[7] M. B. Pillai, S. Nakdhamabhorn, K. Borvorntanajanya, and J. Suthakorn, "Enforced acceleration control for DC actuated rescue robot," in *Proc. XXII Int. Conf. Electr. Mach. (ICEM)*, Sep. 2016, pp. 2640–2648.

[8] A. Abuelnaga, M. Narimani, and A. S. Bahman, "A review on IGBT module failure modes and lifetime testing," *IEEE Access*, vol. 9, pp. 9643–9663, 2021.

[9] B. Siciliano and L. Villani, *Robot Force Control*. Norwell, MA, USA: Kluwer, 1999.

[10] E. Sevinchan, I. Dincer, and H. Lang, "A review on thermal management methods for robots," *Appl. Thermal Eng.*, vol. 140, pp. 799–813, Jul. 2018.

[11] F. Cakmak, E. Uslu, M. F. Amasyali, and S. Yavuz, "Thermal based exploration for search and rescue robots," in *Proc. IEEE Int. Conf. Innov. Intell. Syst. Appl. (INISTA)*, Jul. 2017, pp. 113–118.

[12] F. Rubio, F. Valero, and C. Llopis-Albert, "A review of mobile robots: Concepts, methods, theoretical framework, and applications," *Int. J. Adv. Robotic Syst.*, vol. 16, no. 2, 2019, Art. no. 1729881419839596.

[13] R. R. Murphy, S. Tadokoro, D. Nardi, A. Jacoff, P. Fiorini, H. Choset, and A. M. Erkmen, "Search and rescue robotics," in *Springer Handbook of Robotics*, 2008, pp. 1151–1173.

[14] P. Liljebäck, Ø. Stavdahl, K. Y. Pettersen, and J. T. Gravdahl, "Mamba–A waterproof snake robot with tactile sensing," in *Proc. IEEE/RSJ Int. Conf. Intell. Robots Syst.*, Sep. 2014, pp. 294–301.

[15] Y. Sun, S. Huang, S. Ma, and Q. Quan, "Development of a waterproof servo unit for amphibious robots," in *Proc. IEEE Int. Conf. Cyber Technol. Autom., Control, Intell. Syst. (CYBER)*, Jun. 2015, pp. 923–928.

[16] D. M. Mathew, H. Kattan, C. Weis, J. Henkel, N. Wehn, and H. Amrouch, "Thermoelectric cooling to survive commodity DRAMs in harsh environment automotive electronics," *IEEE Access*, vol. 9, pp. 83950–83962, 2021.

[17] S. Twaha, J. Zhu, Y. Yan, and B. Li, "A comprehensive review of thermoelectric technology: Materials, applications, modelling and performance improvement," *Renew. Sustain. Energy Rev.*, vol. 65, pp. 698–726, Nov. 2016.

[18] D. Zhao and G. Tan, "A review of thermoelectric cooling: Materials, modeling and applications," *Appl. Thermal Eng.*, vol. 66, nos. 1–2, pp. 15–24, May 2014.

[19] M. A. Budiyanto, A. H. Fikri, and H. Ayuningtyas, "Study on the application of thermoelectric coolers inside unmanned surface vehicles," *J. Adv. Res. Fluid Mech. Thermal Sci.*, vol. 82, no. 1, pp. 12–20, Apr. 2021.

[20] H. Morimitsu and S. Katsura, "Heat inflow control of Peltier device based on heat inflow observer," in *Proc. SICE Annu. Conf.*, Aug. 2010, pp. 996–1001.

[21] T. H. Indiketiya, "An optimum strategy to control Peltier device cold side temperature," in *Proc. IEEE 11th Annu. Comput. Commun. Workshop Conf. (CCWC)*, Jan. 2021, pp. 1333–1338.

[22] L. A. Nimmagadda, R. Mahmud, and S. Sinha, "Materials and devices for on-chip and off-chip Peltier cooling: A review," *IEEE Trans. Compon., Packag., Manuf. Technol.*, vol. 11, no. 8, pp. 1267–1281, Aug. 2021.

[23] J. Zhao, K. P. Lam, and B. Erik Ydstie, "EnergyPlus model-based predictive control (EPMPC) by using MATLAB/SIMULINK and MLE+," in *Proc. 13th Conf. Int. Building Perform. Simulation Assoc. (BS)*, 2013, pp. 2466–2473.

[24] C. Li, D. Jiao, J. Jia, F. Guo, and J. Wang, "Thermoelectric cooling for power electronics circuits: Modeling and active temperature control," *IEEE Trans. Ind. Appl.*, vol. 50, no. 6, pp. 3995–4005, Nov./Dec. 2014.

[25] M. Nesarajah and G. Frey, "Thermoelectric power generation: Peltier element versus thermoelectric generator," in *Proc. 42nd Annu. Conf. IEEE Ind. Electron. Soc. (IECON)*, Oct. 2016, pp. 4252–4257.

[26] E. Söylemez, E. Alpman, A. Onat, and S. Hartomacioğlu, "CFD analysis for predicting cooling time of a domestic refrigerator with thermoelectric cooling system," *Int. J. Refrigeration*, vol. 123, pp. 138–149, Mar. 2021.

[27] D. F. Sinulingga, F. M. Prasetyawati, F. M. Palebangan, A. Suhendi, T. A. Ajiwiguna, I. P. Handayani, and I. W. Fathonah, "PID temperature controlling of thermoelectric based cool box," in *Proc. Int. Conf. Control, Electron., Renew. Energy Commun. (ICCREC)*, Sep. 2017, pp. 236–240.
[28] M. D. Thakor, S. K. Hadia, and A. Kumar, "Precise temperature control through thermoelectric cooler with PID controller," in *Proc. Int. Conf. Commun. Signal Process. (ICCSP)*, Apr. 2015, pp. 1118–1122.
[29] S. Petryna, "Model predictive control of a thermoelectric-based heat pump," Univ. Ontario Inst. Technol., ON, Canada, Tech. Rep., 2013.
[30] B. R. Mehta and Y. J. Reddy, "Advanced process control systems," in *Industrial Process Automation Systems*, B. R. Mehta and Y. J. Reddy, Eds. Oxford, U.K.: Butterworth-Heinemann, 2015, Ch 19, pp. 547–557.
[31] H. Qian, G. Xu, J. Yan, T. Lun Lam, Y. Xu, and K. Xu, "Energy management for four-wheel independent driving vehicle," in *Proc. IEEE/RSJ Int. Conf. Intell. Robots Syst.*, Oct. 2010, pp. 5532–5537.
[32] S. Xie, H. He, and J. Peng, "An energy management strategy based on stochastic model predictive control for plug-in hybrid electric buses," *Appl. Energy*, vol. 196, pp. 279–288, Jun. 2017.
[33] N. Wang, Z. Liu, C. Ding, J. Zhang, G. Sui, H. Jia, and X. Gao, "Hight efficiency thermoelectric temperature control system with improved proportional integral differential (PID) algorithm using energy feedback technique," *IEEE Trans. Ind. Electron.*, early access, May 26, 2021, doi: 10.1109/TIE.2021.3082462.
[34] J. Suthakorn, S. Ongwattanakul, C. Moonjaita, P. Owatchaiyapong, P. Thiuthipsakul, K. Borvorntanajanya, S. Chalongwongse, B. M. Pillai, M. Chatrasingh, and N. Nillahoot, "RoboCup rescue 2016 team description paper BART LAB rescue robotics team (Thailand)," RoboCup, Rescue Robot League, Leipzig, Germany, Tech. Rep., 2016.
[35] B. Sharma, B. M. Pillai, and J. Suthakorn, "Live displacement estimation for rough terrain mobile robot: BART LAB rescue robot," in *Proc. Int. Siberian Conf. Control Commun. (SIBCON)*, May 2021, pp. 1–6.
[36] R. Phuengsuk and J. Suthakorn, "A study on risk assessment for improving reliability of rescue robots," in *Proc. IEEE Int. Conf. Robot. Biomimetics (ROBIO)*, Dec. 2016, pp. 667–672.
[37] P. Sattayasoonthorn and J. Suthakorn, "Battery management for rescue robot operation," in *Proc. IEEE Int. Conf. Robot. Biomimetics (ROBIO)*, Dec. 2016, pp. 1227–1232.
[38] J. M. Gonzalez-Gonzalez, A. Trivino-Cabrera, and J. A. Aguado, "Model predictive control to maximize the efficiency in EV wireless chargers," *IEEE Trans. Ind. Electron.*, vol. 69, no. 2, pp. 1244–1253, Feb. 2022.
[39] F. Wang, X. Mei, J. Rodriguez, and R. Kennel, "Model predictive control for electrical drive systems-an overview," *CES Trans. Elect. Mach. Syst.*, vol. 1, no. 3, pp. 219–230, Sep. 2017.
[40] L. Wang, *Model Predictive Control: Design and Implementation Using MATLAB (T-3)*. London, U.K.: Springer, 2009.
[41] E. F. Camacho and C. Bordons, *Model Predictive Control*. London, U.K.: Springer, 2007.
[42] J. A. Rossiter, *Model-Based Predictive Control: A Practical Approach*, 1st ed. Boca Raton, FL, USA: CRC Press, 2005.
[43] *Ansys Fluent 12.0 Theory Guide*, ANSYS FLUENT Release, ANSYS, Canonsburg, PA, USA, 2009.
[44] E. E. Antonova and D. C. Looman, "Finite elements for thermoelectric device analysis in ANSYS," in *Proc. 24th Int. Conf. Thermoelectrics (ICT)*, Jun. 2005, pp. 215–218.

MAYUR KISHORE received the master's degree in industrial refrigeration and cryogenics from the TKM College of Engineering, Kerala, India. He is currently pursuing the Ph.D. degree with the Center for Biomedical and Robotics Technology (BART LAB), Department of Biomedical Engineering, Faculty of Engineering, Mahidol University, Thailand. His research interests include CFD simulations of real-time scenarios, medical robotics, and rescue robotics.

BIBHU SHARMA received the B.E. degree from the School of Engineering, Kathmandu University, Nepal. He is currently pursuing the master's degree with the Center of Biomedical and Robotics Technology (BART LAB), Department of Biomedical Engineering, Faculty of Engineering, Mahidol University, Thailand. He has been involved with research pertaining to medical robotics, biomechanics, and rough-terrain robotics along the direction of design, dynamics, and control.

BRANESH M. PILLAI (Member, IEEE) received the bachelor's degree from Anna University, India, in 2007, the master's degree by research in control systems from the University of Moratuwa, in 2013, and the Ph.D. degree in biomedical engineering (medical robotics) from Mahidol University, Thailand, in 2019. He is currently a Faculty Member at the Center for Biomedical and Robotics Technology (BART LAB), Faculty of Engineering, Mahidol University. His research interests include medical robotics and the work-related to robot-assisted surgery, advanced motion control, biomechanics, and rough terrain rescue robot.

JACKRIT SUTHAKORN (Member, IEEE) received the bachelor's degree in mechanical engineering from Mahidol University, Thailand, in 1995, the master's degree in control engineering from Michigan Technological University, USA, in 1998, and the Ph.D. degree in robotics from Johns Hopkins University, USA, in 2003. He had established the Center for Biomedical and Robotics Technology (BART LAB), the first Interdisciplinary Research Laboratory, Faculty of Engineering, Mahidol University, in 2004. In 2006, he and his colleagues established the Department of Biomedical Engineering, Mahidol University. He was the first BME Department Chair and remained, until 2015. Since 2015, he has been the Dean of the Faculty of Engineering, Mahidol University. He is currently the President leading the Council of Engineering Deans of Thailand. He was one of the founders of Thai Robotics Society (TRS), in 2004, and the President, from 2007 to 2010. He also serves as a Trustee for the International RoboCup Federation, and the Vice President for the RoboCup Asia-Pacific (RCAP). His research interests include medical robotics and field robotics: surgical robotics in various applications, rehabilitation robotics, hospital service and tele-medicine robotics, and rough terrain rescue robotics.